Neural Computing and Applications (2021) 33:17287–17302
https://doi.org/10.1007/s00521-021-06318-7

ORIGINAL ARTICLE

Solution of novel multi-fractional multi-singular Lane–Emden model using the designed FMNEICS

Zulqurnain Sabir[1] · Muhammad Asif Zahoor Raja[2] · Juan L. G. Guirao[3,4] · Tareq Saeed[4]

Received: 24 January 2021 / Accepted: 6 July 2021 / Published online: 27 July 2021
© The Author(s), under exclusive licence to Springer-Verlag London Ltd., part of Springer Nature 2021

Abstract
The present study is related to design a novel multi-fractional multi-singular Lane–Emden model (MFMS-LEM) by keeping the ideas of the literature LEM and by extension of the work of doubly singular multi-fractional LEM. This mathematical novel MFMS-LEM is numerically treated by applying the fractional Meyer neuro-evolution intelligent solver (FMNEICS). The optimization is performed using the mutual heuristics of fractional Mayer wavelet neural networks (FMW-NN), the global search aptitude of genetic algorithms (GAs) and interior-point algorithm (IPA), i.e., FMW-NN-GAIPA. The derivation steps, details of the singular points, fractional terms, shape factors and singular points are also provided. The modeling strength of MW-NN is implemented to characterize the novel model in the sagacity of mean squared error of objective function and network optimization is performed with the integrated capability of GAIPA. The authentication, perfection and verification of FMNEICS is checked for three diverse cases of the novel model which are conventional via relative studies through the reference solutions based on accuracy, stability, robustness and convergence procedures. Furthermore, the explanations via the statistical measures validate the value of the designed stochastic solver FMW-NN-GAIPA.

Keywords Artificial neural networks · Multi-fractional model based on Lane–Emden · Multi-singular systems · Mayer wavelet neural networks · Interior-point algorithm · Genetic algorithms

✉ Juan L. G. Guirao
juan.garcia@upct.es; jlgarcia@kau.edu.sa

Zulqurnain Sabir
zulqurnain_maths@hu.edu.pk

Muhammad Asif Zahoor Raja
rajamaz@yuntech.edu.tw

Tareq Saeed
tsalmalki@kau.edu.sa

1 Department of Mathematics and Statistics, Hazara University, Mansehra, Pakistan

2 Future Technology Research Center, National Yunlin University of Science and Technology, 123 University Road, Section 3, Douliou, Yunlin 64002, Taiwan, R.O.C.

3 Department of Applied Mathematics and Statistics, Technical University of Cartagena, Hospital de Marina, 30203 Cartagena, Spain

4 Nonlinear Analysis and Applied Mathematics (NAAM)-Research Group, Department of Mathematics, Faculty of Science, King Abdulaziz University, P.O. Box 80203, Jeddah 21589, Saudi Arabia

1 Introduction

The system based on fractional order signified with differential equations of fractional order and integer terms have been widely deliberated due to the numerous applications in control systems, physics, engineering and mathematical sciences. The study of fractional calculus involving different operatives has become one of the most valuable and interesting topics for the research community during the last thirty years. To mention some operators, have supreme significance are the Caputo operator [1], Erdelyi–Kober operator [2], Weyl–Riesz operator [3], Riemann–Liouville [5] and Grunwald–Letnikov operator [5]. Keeping the ideas of these fractional-based operatives, the researchers are interested to investigate these operators in different fields like as fractional viscoplasticity modeling [6–8], parameter estimation problem for input nonlinear control autoregressive systems [9], dynamical studies of earth systems [10], reactive power planning involving FACTS devices [11], edge exposure in road hurdle [12], reactive power flow systems [13], reaction problem of surface–volume [14], optimization of reactive power dispatch problems [15], behaviors study in the real ingredients [16], power signals parameter estimation [17], modeling of viscoelastic systems [18], power systems [19], theory of electromagnetic established on the concepts of fractional calculus [20], higher order models based on singular points [21], nanofluids-based mathematical models [22], mathematical models for tiny hardware implants [23], LC-electric circuit fractal models [24], financial market forecasting [25], physics [26], nuclear engineering [27], control systems [28], recommender systems [29], engineering-based dynamics [30], system identification [31] and some other fields, see [32–35].

Several singular studies are found in the literature that are always difficult to solve using the conventional/traditional analytical and numerical schemes, in which one of the famous studies is Lane–Emden singular system (LESS). The LESS is a historical model and has many applications like astrophysics, spherical cloud of gas and quantum mechanics. The LESS is famous due to the involvement of singularity at the origin. There are many numerical schemes that have been implemented to solve this famous LESS [36–42]. The generic form of the LESS is given as [43–45]:

$$\begin{cases} \frac{d^2S}{dy^2} + \frac{u}{y}\frac{dS}{dy} + h(S) = p(y), \\ S(0) = a_1, \frac{dS(0)}{dy} = a_2. \end{cases} \tag{1}$$

The singularity appears on $y = 0$ and the value of the shape vector is $u \geq 1$. The idea of the present study is to construct a multi-fractional multi-singular Lane–Emden model (MFMS-LEM) that comes in the mind by generalizing the LESS and the extension of the work of Sabir et al. [46]. The following mathematical steps have been applied as [47]:

$$y^{-v}\frac{d^f}{dy^f}\left(y^v \frac{d^g}{dy^g}\right)S(y) + h(S) = p(y), \tag{2}$$

where v shows a positive real valued number and $p(y)$ is a forcing function. For the derivation of the MFMS-LEM, the values of f and p can be chosen as:

$$f = 3, \quad p = \alpha, \text{ where } 0 < \alpha < 1. \tag{3}$$

Equation (2) is updated using the above equation as follows:

$$y^{-v}\frac{d^3}{dy^3}\left(y^v \frac{d^\alpha}{dy^\alpha}\right)S(y) + h(S) = p(y). \tag{4}$$

The simplified form of the above equation is written as:

$$\begin{aligned} \frac{d^3}{dy^3}\left(y^v \frac{d^\alpha}{dy^\alpha}\right)S(y) = x^u \frac{d^{\alpha+3}}{dy^{\alpha+3}}S(y) + 3vy^{v-1}\frac{d^{\alpha+2}}{dy^{\alpha+2}}S(y) \\ + 3v(v-1)y^{v-2}\frac{d^{\alpha+1}}{dy^{\alpha+1}}S(y) \\ + v(v-1)(v-2)y^{v-3}\frac{d^\alpha}{dy^\alpha}S(y). \end{aligned} \tag{5}$$

Hence, the obtained form of the mathematical model becomes as:

$$\begin{cases} \frac{d^{\alpha+3}}{dy^{\alpha+3}}S(y) + \frac{3v}{y}\frac{d^{\alpha+2}}{dy^{\alpha+2}}S(y) + \frac{3v(v-1)}{y^2}\frac{d^{\alpha+1}}{dy^{\alpha+1}}S(y) \\ + \frac{v(v-1)(v-2)}{y^3}\frac{d^\alpha}{dy^\alpha}S(y) + h(S) = p(y), \\ S(0) = 0, \quad S(0.5) = A, \quad S(1) = B. \end{cases} \tag{6}$$

The obtained mathematical form of the model provided in the above equation is named as MFMS-LEM. The shape factor values are $3v$, $3v(v-1)$ and $v(v-1)(v-2)$, respectively, whereas the singularity appears three times at the variables y, y^2 and y^3 in the 2nd, 3rd and 4th terms, respectively. Moreover, α shows the fractional order and it appears four times as α, $\alpha+1$, $\alpha+2$ and $\alpha+3$. The third and fourth terms vanish for $v = 1$ and shape factor reduces to 3. The further mathematical details for deriving such system can be seen in [46].

1.1 Problem statement and associated work

The purpose of the current work is to form a MFMS-LEM and numerically investigated by the stochastic computing technique for solving the MFMS-LEM defined in Eq. (6) using the fractional Mayer wavelet neural networks (FMW-NN) under the optimization of global search effectiveness of genetic algorithms (GAs) and interior-point algorithm (IPA), i.e., FMW-NN-GAIPA. The meta-heuristic-based intelligent computing solvers have been broadly implemented to analyze the singular/non-singular, linear/nonlinear and biological models using neural networks using the optimization of swarming/evolutionary computing approaches [48–55]. Few relevant potential equations include seasonal groundwater table depth prediction [56], optimization of power dispatch problems representing Algerian electricity grid [57], aeromechanical optimization of compressor [58], solution of the nonlinear corneal shape model [59], optimization in biodiesel production [60], solving the nonlinear electrical circuit models [61], forecasting of streamflow discharges [62], parameter estimation problems of power signal models [63], estimation of the soil temperature [64], optimization of electrically stimulated muscle models [65], prediction of rainfall time series [66] and attenuation of noise interferences [67]. The authors are inspired based on these operative contributions to design the computing numerical solver for solving the MFMS-LEM.

1.2 Novelty and contribution

The originality of the current work is itemized as follows as:

- A novel MFMS-LEM is considered using the sense of typical LESS and numerically solved by using a novel design of FMNEICS that have been considered by the fractional Mayer wavelet neural networks using the optimization of global search competence of GAs aided with local rapid search of IPA.
- The obtained numerical outcomes of the newly designed MFMS-LEM are compared using the FMNEICS from accessible exact/true results that validate its correctness, stability and convergence.
- The reliable performance of the designed FMNEICS is further enhanced via the statistical studies in terms of Nash Sutcliffe efficiency (NSE), root-mean-square error (R.MSE), semi-interquartile range (S.I.R) and Theil's inequality coefficient (TIC) measures.
- Beside the soundly accurate results for the MFMS-LEM by the FMNEICS, smooth operations, ease of understanding, exhaustive applicability and robustness are other valued compensations.

1.3 Organization of the work

The other parts of this paper are concisely labeled as: The designed approach is presented in Sect. 2 to solve the MFMS-LEM. The mathematical steps for the performance measures are defined in Sect. 3. The comprehensive outcomes to solve the projected model are provided in Sect. 4 and the conclusion along with the future research details are provided in the last Sect.

2 Methodology based on the FMNEICS

This current section is associated with the material accessible for FMNEICS-based computing intelligent solver and execution process for the MFMS-LEM using the FMW-NN-along with the Mayer wavelet functions. The structure for designing the error-based merit function, system of differential equations and the optimization procedure using the GAIPA are introduced elaborative in this section.

2.1 Merit function: FMWNN

The models based on ANN are implemented to provide the numerical results of numerous fractional order models [68–70]. In this procedure, $\hat{S}(y)$ shows the proposed solution of the system model, $D^{\alpha}\hat{S}(y)$ and $D^{(n)}\hat{S}(y)$ show the respective form of the fractional α^{th} and n^{th} order derivatives. The terminologies of these network systems in the form of continuous mapping are shown as:

$$\begin{aligned}\hat{S}(y) &= \sum_{i=1}^{j} b_i \rho(w_i y + q_i),\\ D^{\alpha}\hat{S}(y) &= \sum_{i=1}^{j} b_i D^{\alpha}\rho(w_i y + q_i),\\ D^{(n)}\hat{S}(y) &= \sum_{i=1}^{j} b_i D^{(n)}\rho(w_i y + q_i),\end{aligned} \tag{7}$$

where, j shows the number of neurons, while $\boldsymbol{b}$, $\boldsymbol{w}$ and $\boldsymbol{q}$ are vector component forms $\boldsymbol{W}$, given as follows:

$\boldsymbol{W} = [\boldsymbol{b}, \boldsymbol{w}, \boldsymbol{q}], \quad \text{for } \boldsymbol{b} = [b_1, b_2, \ldots, b_j],$
$\boldsymbol{w} = [w_1, w_2, \ldots, w_j] \textit{ and } \boldsymbol{q} = [q_1, q_2, \ldots, q_j].$

The activation kernel based on Mayer wavelet function is provided as [46]:

$$\rho(y) = 35y^4 - 84y^5 + 70y^6 - 20y^7. \tag{8}$$

The simplified system (7) form using Eq. (8) is given as follows:

$$\begin{aligned}\hat{S}(y) &= \sum_{i=1}^{j} b_j \left(35(w_j y + q_j)^4 - 84(w_j y + q_j)^5 + 70(w_j y + q_j)^6 - 20(w_j y + q_j)^7\right),\\ D^{\alpha}\hat{S}(y) &= \sum_{i=1}^{j} b_j \begin{pmatrix} 35D^{\alpha}(w_j y + q_j)^4 - 84D^{\alpha}(w_j y + q_j)^5 + 70D^{\alpha}(w_j y + q_j)^6 \\ -20D^{\alpha}(w_j y + q_j)^7 \end{pmatrix},\\ D^{(n)}\hat{S}(y) &= \sum_{i=1}^{j} b_j \begin{pmatrix} 35D^{(n)}(w_j y + q_j)^4 - 84D^{(n)}(w_j y + q_j)^5 + 70D^{(n)}(w_j y + q_j)^6 \\ -20D^{(n)}(w_j y + q_j)^7 \end{pmatrix}.\end{aligned} \tag{9}$$

The arbitrary form of the FMWNN is implemented for solving the novel MFMS-LEM associated with the accessibility of "$\boldsymbol{W}$," i.e., appropriate weight. Furthermore, the fractional order "α" is fixed with care to solve the dynamics of MFMS-LEM as given in Eq. (6). In order to get the approximate ANN weights, one may explore the approximation theory using the mean squared error to get a fitness function ξ as given below:

$$\xi = \xi_1 + \xi_2. \tag{10}$$

Here, ξ_1 and ξ_2 are the merit functions associated with the differential model and the boundary conditions of the novel MFMS-LEM provided in Eq. (6), respectively. These merits function are mathematical defined as:

$$\xi_1 = \frac{1}{N}\sum_{i=1}^{j}\left(\begin{array}{c}\frac{d^{\alpha+3}}{dy^{\alpha+3}}\hat{S}_j + \frac{3v}{y_j}\frac{d^{\alpha+2}}{dx^{\alpha+2}}\hat{S}_j + \frac{3v(v-1)}{y_j^2}\frac{d^{\alpha+1}}{dy^{\alpha+1}}\hat{S}_j \\ +\frac{v(v-1)(v-2)}{y_j^3}\frac{d^{\alpha}}{dy^{\alpha}}\hat{S}_j + h(\hat{S}_j) - p_j\end{array}\right)^2, \tag{11}$$

$$\xi_2 = \frac{1}{2}\left((\hat{S}_0)^2 + (\hat{S}_{0.5} - A)^2 + (\hat{S}_N)^2\right), \tag{12}$$

for

$$\hat{S}_j = \hat{S}(y_j),\ p_j = p(y_j)\ ,\ h(S) = h(\hat{S}_j),\ y_j = jh$$

and $Nh = 1$.

One may regulate to solve the novel MFMS-LEM as shown in Eq. (6) with the obtainability of suitable "$\boldsymbol{W}$," such that, $\xi \to 0$, the estimated form of the results of ANN becomes approximately the same as the ideal/exact solutions, *i.e.,* $[\hat{S} \to S]$.

2.2 Optimization of the network

The parameter-based optimizations for the FMWNN is conducted with the competency of hybrid learning ability of GAIPA, a combination of global and local search methodology, to solve the novel design of MFMS-LEM as shown in Eq. (6).

GAs are an efficient global optimization procedure for constrained/unconstrained problems or tasks that are expressed to the mathematical modeling process using the natural genetic systems. The separate frequent population is updated in GAs, *i.e.,* candidate results of the optimization task and has the competence for solving the numerous optimization systems by merging the reproduction tools via the selection, crossover, operators; mutation and elitism. Recently, GA is used to be exploited to the optimal weight design for the frames of steel space [71], parameter documentation of the nonlinear multivariable models [72], nonlinear Bratu model optimization [73], control construction robot of car model [74], optimization of the layer thickness using the multilayer piezoelectric transducer [75], active noise control systems [76], parameter estimation using the plane waves of electromagnetic [77], solution of nonlinear singular Flierl–Petviashivili systems [78], load dispatch integrated model connecting both wind and thermal generators [79] and dynamics analysis for the model of heartbeat [80]. The indolence and slowness of the GA using the hybridization with the IPA can be promoted during the optimization process.

IPA is a rapid and efficient local search approach for the adjustment of optimization tasks in various submissions in the diversity of areas. IPA fits to well-ordered solvers based on convex optimization, which can be explored for both types of the systems constrained and unconstrained. Some transmuted applications addressed competently by IPA are the image restoration [81], economic load dispatch problems [82], semi-definite programming [83], optimization of noise control system without identification of secondary path [84], onboard powered-descent guidance [85], non-smooth contact dynamics [86] and localization of dynamic forces [87]. The parameter settings of the neurons in FMWNNs, settings of parameters for both GA and IPA algorithms should be done with care, after extensive experimentation and with experience for better performance of FMWNN-GAIPA, a small variation in these parameter results in divergence or trapping into local minimum.

3 Performance measures

Four different performance procedures named as R.MSE, TIC, ENSE and S.I.R are presented to solve the novel MFMS-LEM in this section. These measures are used to verify and validate the worth of the design scheme FMWNN on different parameters for the perfect modeling. The mathematical notations of these measures R.MSE, TIC, ENSE and S.I.R for the true results S and the proposed results $\hat{S}$ are given as:

$$\text{R.MSE} = \sqrt{\frac{1}{n}\sum\nolimits_{i=1}^{j}\left(S_j - \hat{S}_j\right)^2}, \tag{13}$$

$$\text{TIC} = \frac{\sqrt{\frac{1}{n}\sum_{i=1}^{j}\left(S_j - \hat{S}_j\right)^2}}{\left(\sqrt{\frac{1}{n}\sum_{i=1}^{j}S_j^2} + \sqrt{\frac{1}{n}\sum_{i=1}^{j}\hat{S}_j^2}\right)}, \tag{14}$$

$$\text{NSE} = \left\{1 - \frac{\sum_{i=1}^{j}\left(S_j - \hat{S}_j\right)^2}{\sum_{i=1}^{j}\left(S_j - \bar{S}_j\right)^2},\quad \bar{S}_j = \frac{1}{n}\sum_{i=1}^{j}S_j,\right. \tag{15}$$

$$\text{ENSE} = 1 - \text{NSE}, \tag{16}$$

$$\begin{cases} \text{S.I.R} = -0.5 \times (Q_1 - Q_3), \\ Q_1 = 1^{st} \text{ quartile } \& \;\; Q_3 = 3^{rd} \text{ quartile.} \end{cases} \tag{17}$$

4 Results and simulations

In this section, the detail of the numerical results to solve three different variants of the novel MFMS-LEM is presented. Single input/output and the structure of hidden layers using the Mayer neural networks is implemented to model Eq. (6) with the help of networks presented in Eqs. (10–12), whereas the Matlab build package for "optimization" toolbox is exploited to train the weights of FMWNN models to solve the MFMS-LEM using "GA" together with "fmincon" routine of algorithm "IPA." The numerical results of the proposed FMWNN using the GAIPA for sixty independent runs are drawn to solve the novel MFMS-LEM and outcomes are portrayed with sufficient numerical as well as graphical presentation to assess the accuracy and convergence.

Example 1 Consider the MFMS-LEM shown in the model (6) after multiplying by y^3 for both sides is given as:

$$\begin{cases} y^3 \dfrac{d^{\alpha+3}}{dy^{\alpha+3}} S(y) + 3y^2 \dfrac{d^{\alpha+2}}{dy^{\alpha+2}} S(y) + 3v(v-1)y \dfrac{d^{\alpha+1}}{dy^{\alpha+1}} S(y) \\ + v(v-1)(v-1) \dfrac{d^{\alpha}}{dy^{\alpha}} S(y) + y^3 h(S) = y^3 p(y) = j(y), \\ S(0) = 0, \;\; S(0.5) = A, \;\; S(1) = B. \end{cases} \tag{18}$$

where,

$$\begin{aligned} j(y) = y^{l+3} - y^{r+3} + y^3 & \\ & \left(\frac{\Gamma(l+1)}{\Gamma(l-\alpha-2)} y^{l-\alpha-3} - \frac{\Gamma(r+1)}{\Gamma(r-\alpha-2)} x^{r-\alpha-3} \right) \\ & + 9y^2 \left(\frac{\Gamma(l+1)}{\Gamma(l-\alpha-1)} y^{l-\alpha-2} - \frac{\Gamma(r+1)}{\Gamma(r-\alpha-1)} x^{r-\alpha-2} \right) \\ & + 18y \left(\frac{\Gamma(l+1)}{\Gamma(l-\alpha)} y^{l-\alpha-1} - \frac{\Gamma(r+1)}{\Gamma(r-\alpha)} y^{r-\alpha-1} \right) \\ & + 6 \left(\frac{\Gamma(l+1)}{\Gamma(l-\alpha+1)} y^{l-\alpha} - \frac{\Gamma(r+1)}{\Gamma(r-\alpha+1)} y^{r-\alpha} \right). \end{aligned} \tag{19}$$

Here the l and r values are taken as positive.

The simplified form of Eq. (18) using Eq. (19) is written as:

$$\begin{cases} y^3 \dfrac{d^{\alpha+3}}{dy^{\alpha+3}} S(y) + 3y^2 \dfrac{d^{\alpha+2}}{dy^{\alpha+2}} S(y) + 3v(v-1)y \dfrac{d^{\alpha+1}}{dy^{\alpha+1}} S(y) \\ + v(v-1)(v-1) \dfrac{d^{\alpha}}{dy^{\alpha}} S(y) + h(S) \\ = y^{l+3} - y^{r+3} \\ + y^3 \left(\dfrac{\Gamma(l+1)}{\Gamma(l-\alpha-2)} y^{l-\alpha-3} - \dfrac{\Gamma(r+1)}{\Gamma(r-\alpha-2)} x^{r-\alpha-3} \right) \\ + 9y^2 \left(\dfrac{\Gamma(l+1)}{\Gamma(l-\alpha-1)} y^{l-\alpha-2} - \dfrac{\Gamma(r+1)}{\Gamma(r-\alpha-1)} x^{r-\alpha-2} \right) \\ + 18y \left(\dfrac{\Gamma(l+1)}{\Gamma(l-\alpha)} y^{l-\alpha-1} - \dfrac{\Gamma(r+1)}{\Gamma(r-\alpha)} y^{r-\alpha-1} \right) \\ + 6 \left(\dfrac{\Gamma(l+1)}{\Gamma(l-\alpha+1)} y^{l-\alpha} - \dfrac{\Gamma(r+1)}{\Gamma(r-\alpha+1)} y^{r-\alpha} \right) \\ S(0) = 0, \;\; S(0.5) = -0.0313, \;\; S(1) = 0. \end{cases}$$

The true solution of the MFMS-LEM given in Eq. (20) is shown as:

$$S(y) = y^l - y^r. \tag{21}$$

For the particular values of $l = 5$ and $r = 4$, the updated form of the exact solutions is given as:

$$S(y) = y^5 - y^4. \tag{22}$$

The merit function for Eq. (20) is designed as:

$$\xi = \frac{1}{N} \sum_{i=1}^{j} \begin{pmatrix} y_j^3 \dfrac{d^{\alpha+3}}{dy_j^{\alpha+3}} \hat{S}_j + 9y_j^2 \dfrac{d^{\alpha+2}}{dy_j^{\alpha+2}} \hat{S}_j + 18y_j \dfrac{d^{\alpha+1}}{dy_j^{\alpha+1}} \hat{S}_j \\ +6 \dfrac{d^{\alpha}}{dy_j^{\alpha}} \hat{S}_j + y_j^3 h(\hat{S}_j) - y_j^{l+3} + y_j^{r+3} \\ -y_j^3 \left(\dfrac{720}{\Gamma(3-\alpha)} y^{2-\alpha} - \dfrac{120}{\Gamma(2-\alpha)} y^{1-\alpha} \right) \\ -9y_j^2 \left(\dfrac{720}{\Gamma(4-\alpha)} y^{3-\alpha} - \dfrac{120}{\Gamma(3-\alpha)} y^{2-\alpha} \right) \\ -18y_j \left(\dfrac{720}{\Gamma(5-\alpha)} y^{4-\alpha} - \dfrac{120}{\Gamma(3-\alpha)} y^{3-\alpha} \right) \\ -6 \left(\dfrac{720}{\Gamma(6-\alpha)} y^{5-\alpha} - \dfrac{120}{\Gamma(5-\alpha)} y^{4-\alpha} \right) \end{pmatrix}^2 + \frac{1}{3} \left(\left(\hat{S}_0\right)^2 + \left(\hat{S}_{0.5} + 0.0313\right)^2 + \left(\hat{S}_N\right)^2 \right). \tag{23}$$

Three MFMS-LEM cases are considered for different α values, i.e., $\alpha = 0.1$, 0.2 and 0.3. In order to find the performance of these three cases of the presented MFMS-LEM, the optimization through the hybrid combination of GAIPA using the global/ local search capabilities is performed. The whole procedure repeats for a sixty independent runs to produce a larger dataset based on the parameters of ANN. The mathematical terminologies attained by one optimized parameter sets of proposed FMWNN-GAIPA for all cases of the novel MFMS-LEM are provided as:

$$\begin{aligned}\hat{S}_{C-1} = &-0.132\Big(35(0.035y-0.5497)^4-84(0.035y-0.5497)^5+70(0.035y-0.5497)^6-20(0.035y-0.5497)^7\Big)\\&-8.4655\Big(35(0.0008y-0.153)^4-84(0.0008y-0.153)^5+70(0.0008y-0.153)^6-20(0.0008y-0.153)^7\Big)\\&+0.9463\Big(35(-0.156y-0.195)^4-84(-0.156y-0.195)^5+70(-0.156y-0.195)^6-20(-0.156y-0.195)^7\Big)\\&+\cdots-0.3233\Big(35(1.2929y-0.317)^4-84(1.2929y-0.317)^5+70(1.2929y-0.317)^6-20(1.2929y-0.317)^7\Big),\end{aligned}\tag{24}$$

$$\begin{aligned}\hat{S}_{C-2} = &\,0.7991\Big(35(0.1437y+1.0243)^4-84(0.1437y+1.0243)^5+70(0.1437y+1.0243)^6-20(0.1437y+1.0243)^7\Big)\\&-2.5483\Big(35(0.3447y+0.7363)^4-84(0.3447y+0.7363)^5+70(0.3447y+0.7363)^6-20(0.3447y+0.7363)^7\Big)\\&+0.0010\Big(35(-1.291y+2.0509)^4-84(-1.291y+2.0509)^5+70(-1.291y+2.0509)^6-20(-1.291y+2.0509)^7\Big)\\&+\cdots+7.9045\Big(35(-0.181y+0.0370)^4-84(-0.181y+0.0370)^5+70(-0.181y+0.0370)^6\\&-20(-0.181y+0.0370)^7\Big),\end{aligned}\tag{25}$$

$$\begin{aligned}\hat{S}_{C-3} = &-0.101\Big(35(-0.086y-0.124)^4-84(-0.086y-0.124)^5+70(-0.086y-0.124)^6-20(-0.086y-0.124)^7\Big)\\&-0.0003\Big(35(1.2639y-0.825)^4-84(1.2639y-0.825)^5+70(1.2639y-0.8252)^6-20(1.2639y-0.8252)^7\Big)\\&+0.1400\Big(35(-0.452y+0.002)^4-84(-0.452y+0.002)^5+70(-0.452y+0.002)^6-20(-0.452y+0.002)^7\Big)\\&+\cdots+0.0043\Big(35(-0.213y+0.455)^4-84(-0.213y+0.455)^5+70(-0.213y+0.455)^6\\&-20(-0.213y+0.455)^7\Big).\end{aligned}\tag{26}$$

Equations (24–26) represent the proposed numerical outcomes and the plots for all the cases of the novel MFMS-LEM are provided in Fig. 1, particularly subfigures (a-c). The comparison plots of the best, worst and mean results are provided in Fig. 1, particularly subfigures (d-f) for each case of the MFMS-LEM. It is observed in the figures that the values for the best, worst and mean results are overlapped consistently. These perfect result comparisons indicate the correctness of the designed approach. The plots of performance measures are also drawn in Fig. 1, particularly in subfigure (g) for all cases of the MFMS-LEM. One can understand that the values-based performance for RMSE on the basis of the best results for cases 1, 2 and 3 lie around 10^{-05} to 10^{-06}, the TIC values are found around 10^{-09} to 10^{-10}. The ENSE values for case 1 are found around 10^{-08} to 10^{-09}, while the other two cases for ENSE values lie around 10^{-09} to 10^{-10}. One can easily claim that the calculated results based on these performance measures are accurate and thus show very good performance for solving all the cases of the MFMS-LEM. The best values of the absolute error (AE) for solving all

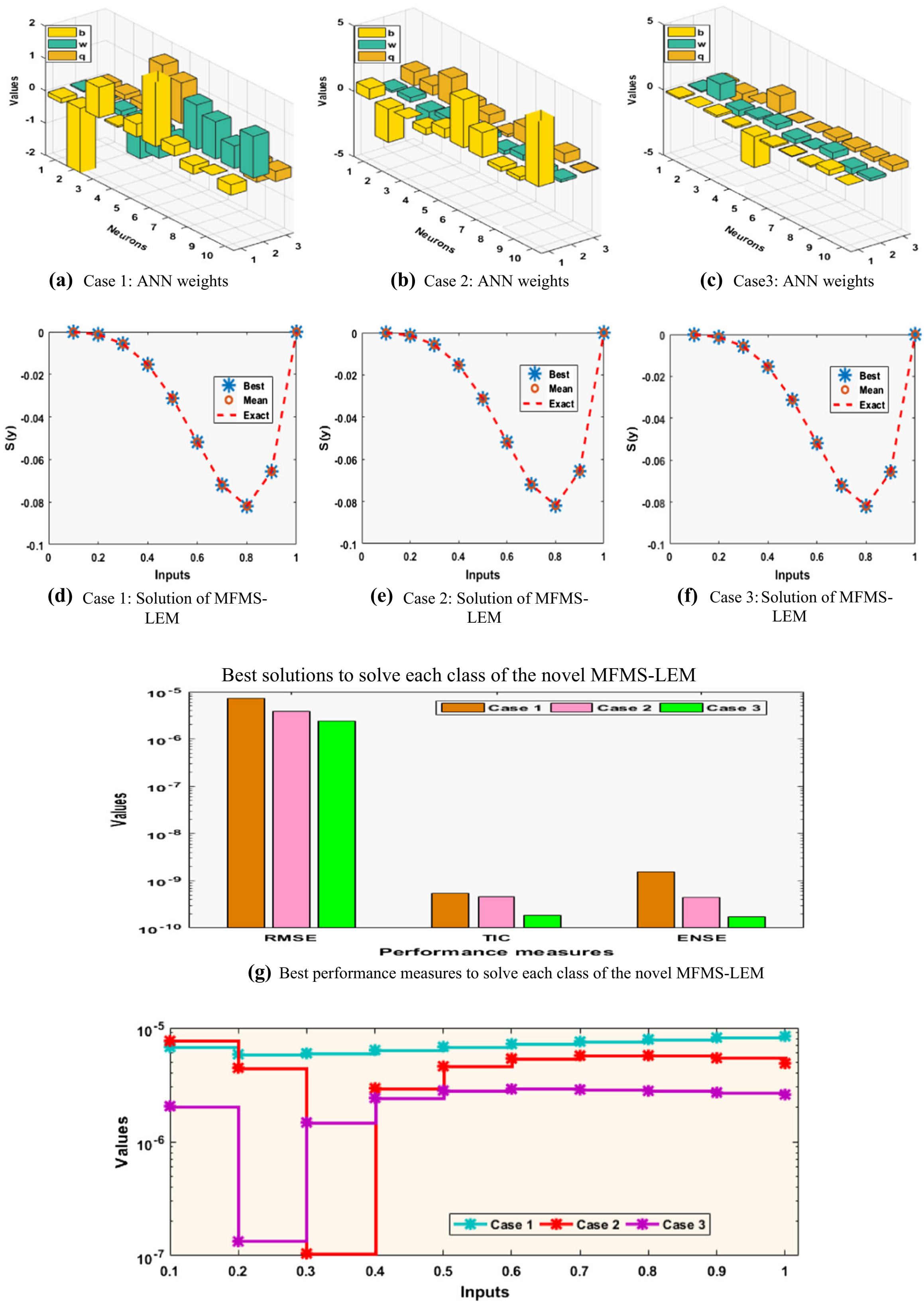

(a) Case 1: ANN weights

(b) Case 2: ANN weights

(c) Case3: ANN weights

(d) Case 1: Solution of MFMS-LEM

(e) Case 2: Solution of MFMS-LEM

(f) Case 3: Solution of MFMS-LEM

(g) Best performance measures to solve each class of the novel MFMS-LEM

(h) Best AE values to solve each class of the novel MFMS-LEM

Fig. 1 Result plots, **a–c** for the trained weights, approximate solutions (**d–f**), best performance measures (**h**) and AE best values (**g**) to solve each class of novel MFMS-LEM

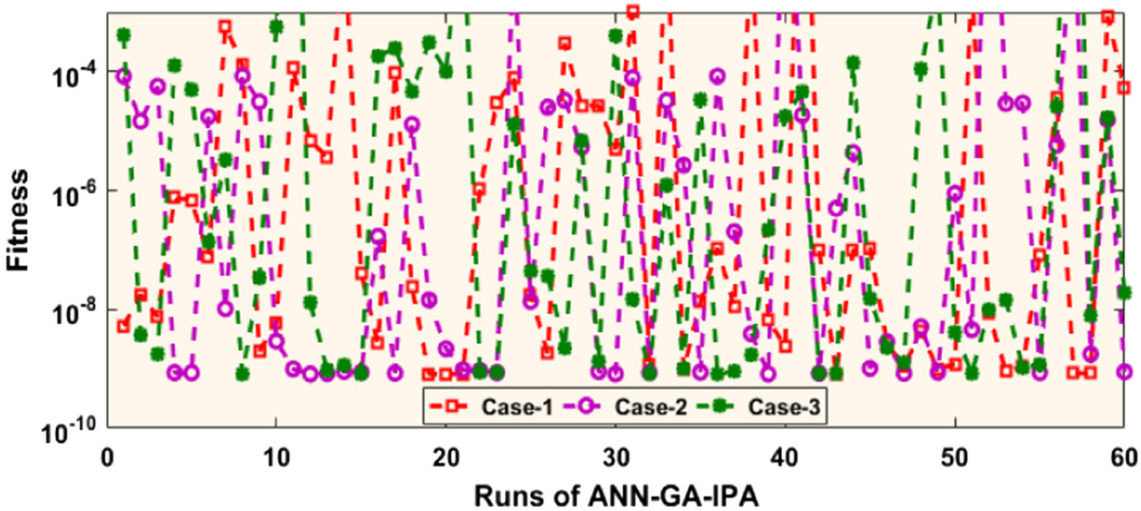

Convergence procedures for each class of the MFMS-LEM using the FIT on y-axis and independent executions of projected FMWNN-GAIPA on x-axis

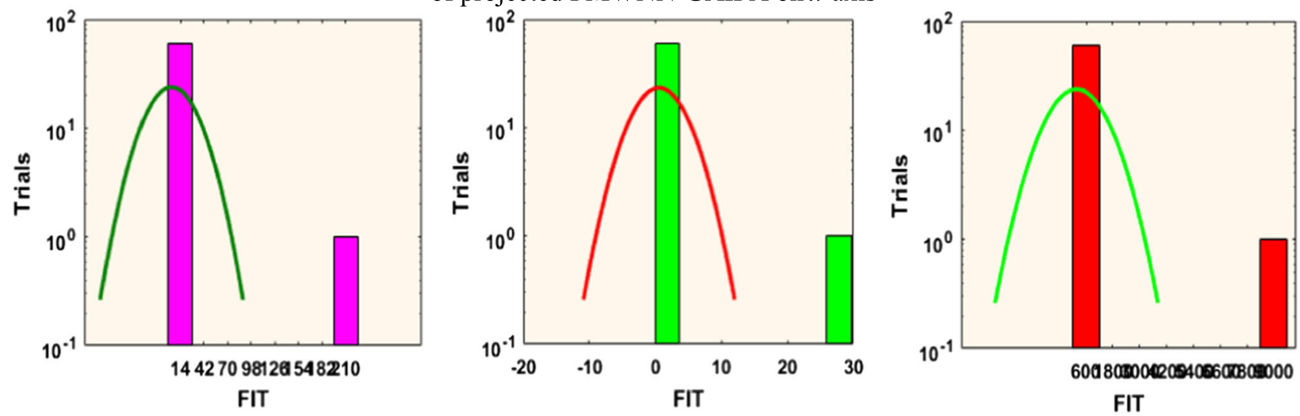

(a) Case-1: Hist values of Fitness **(b)** Case-2: Hist values of Fitness **(c)** Case-3: Hist values of Fitness

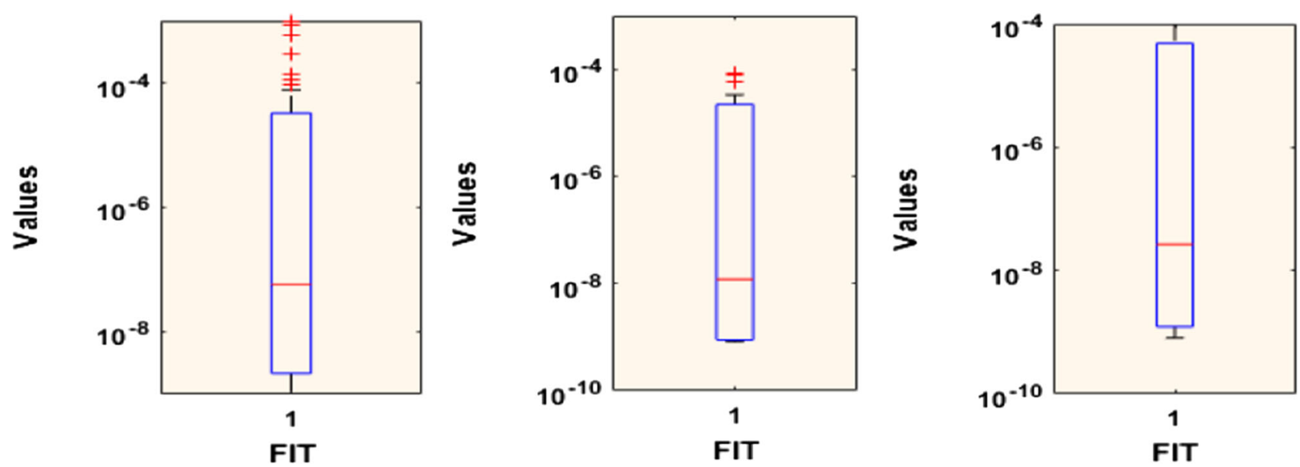

(d) Case-1: Fitness boxplot values **(e)** Case-2: Fitness boxplot values **(f)** Case-3: Fitness boxplot values

Fig. 2 Convergence plots for all cases of the MFMS-LEM for the Fitness together with the boxplots and histograms and 10 neurons

cases of the novel MFMS-LEM is plotted in Fig. 1, particularly in subfigure (h). It is seen that most of the AE values for all cases of the novel MFSE-LEM lie around 10^{-05} to 10^{-07} that indicate the correctness of the designed ANN-GA-IPA scheme.

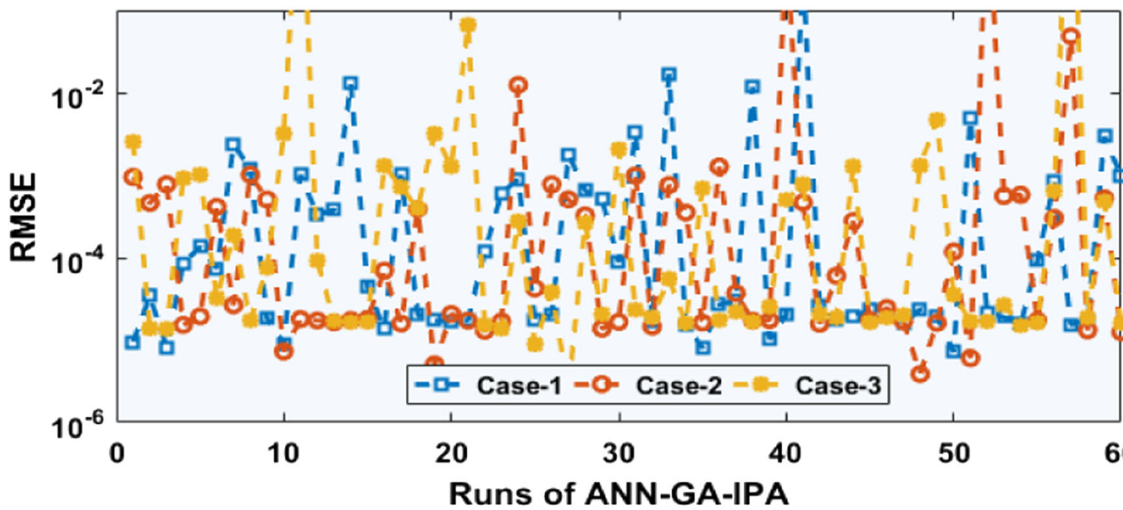

Convergence procedures of the MFMS-LEM using the RMSE on *y*-axis and independent executions of FMWNN-GAIPA on *x*-axis

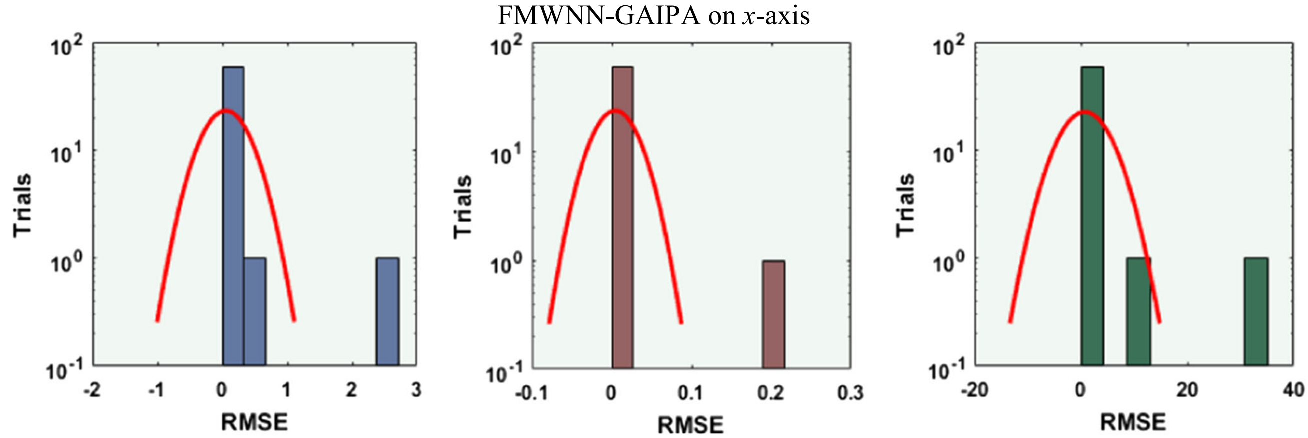

(a) Case-1: Hist RMSE values **(b)** Case-2: Hist RMSE values **(c)** Case-3: Hist RMSE values

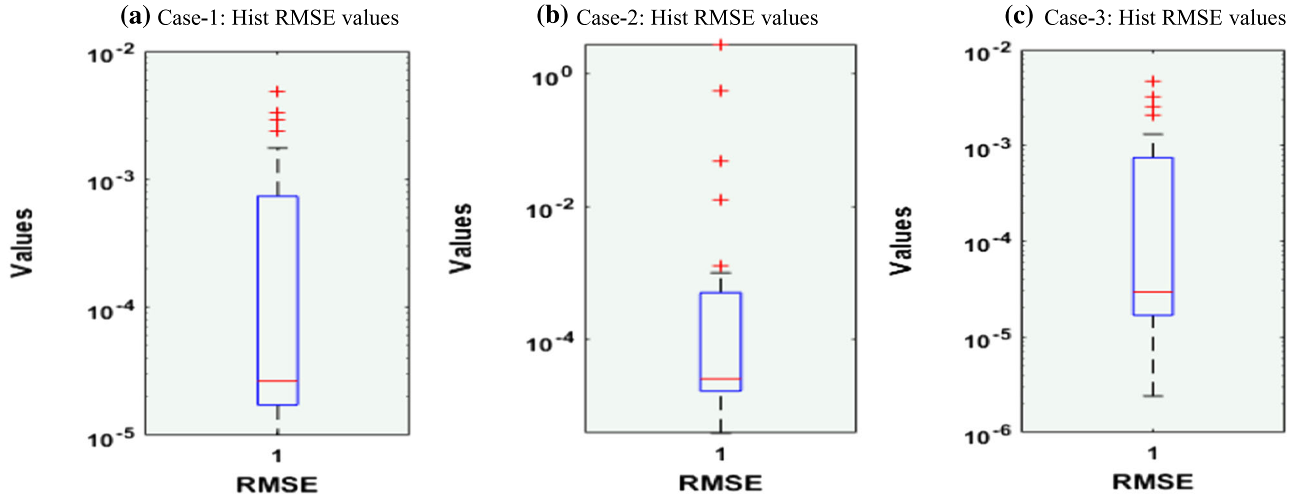

(d) Case-1: RMSE boxplot values **(e)** Case-2: RMSE boxplot values **(f)** Case-3: RMSE boxplot values

Fig. 3 Convergence plots of the MFMS-LEM using the RMSE together with the boxplots and histograms and 10 neurons

The statistical performance values based on the fitness, RMSE, TIC and ENSE gages together with the histograms/boxplots values are shown in Figs. 2, 3, 4 and 5. The results presented in Fig. 2 indicate the performance of the fitness

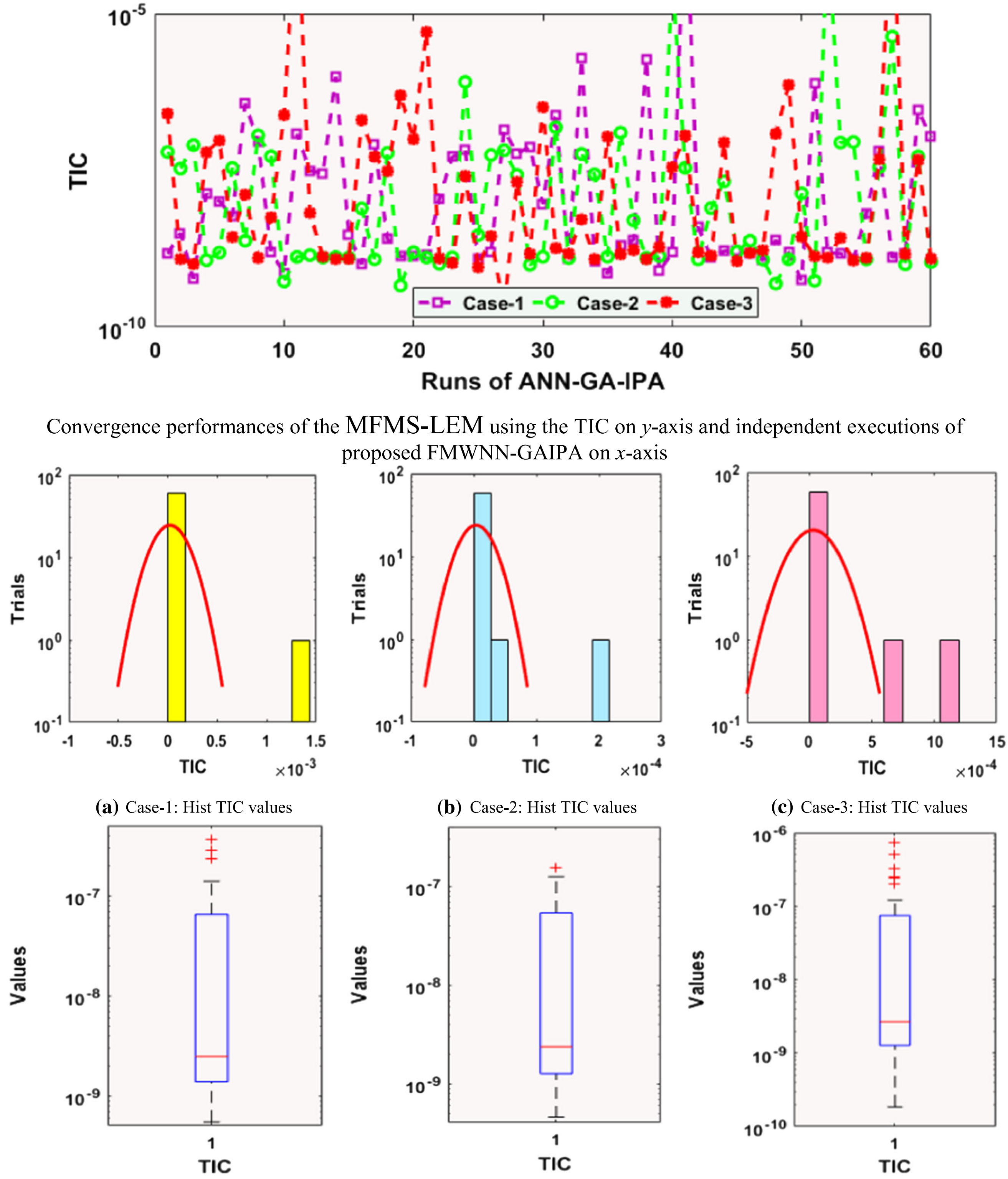

Convergence performances of the MFMS-LEM using the TIC on *y*-axis and independent executions of proposed FMWNN-GAIPA on *x*-axis

(a) Case-1: Hist TIC values

(b) Case-2: Hist TIC values

(c) Case-3: Hist TIC values

(d) Case-1: TIC boxplot values

(e) Case-2: TIC boxplot values

(f) Case-3: TIC boxplot values

Fig. 4 Convergence plots of the MFMS-LEM using the TIC together with boxplots and histograms and 10 neurons

using the novel MFSE-LEM and outcomes show that the majority of the values based on fitness, RMSE, TIC and ENSE found around 10^{-04}—10^{-08}, 10^{-02}—10^{-06}, 10^{-07}—10^{-10} and 10^{-05}—10^{-09} for each case of the novel MFSE-

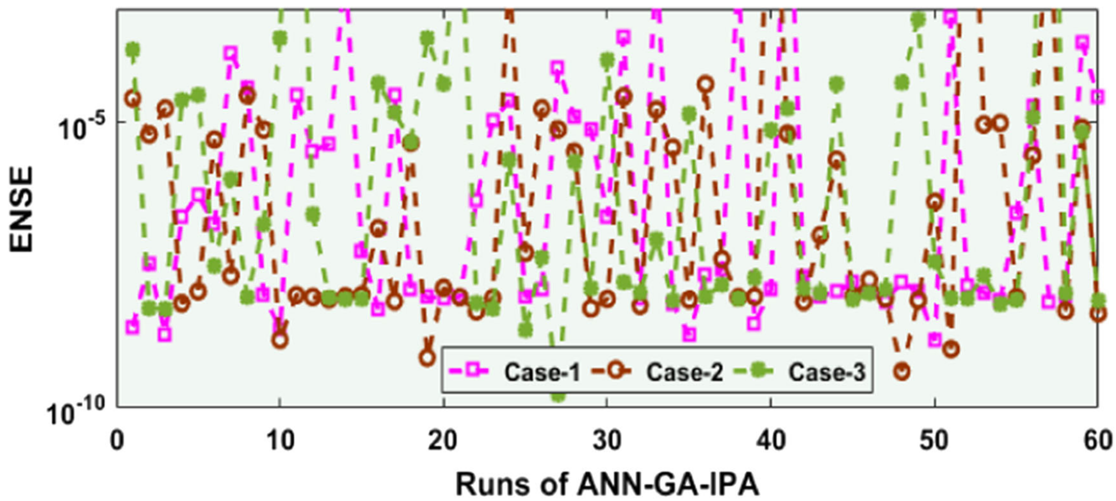

Convergence plots of the MFMS-LEM using the ENSE on y-axis and independent executions of FMWNN-GAIPA on x-axis

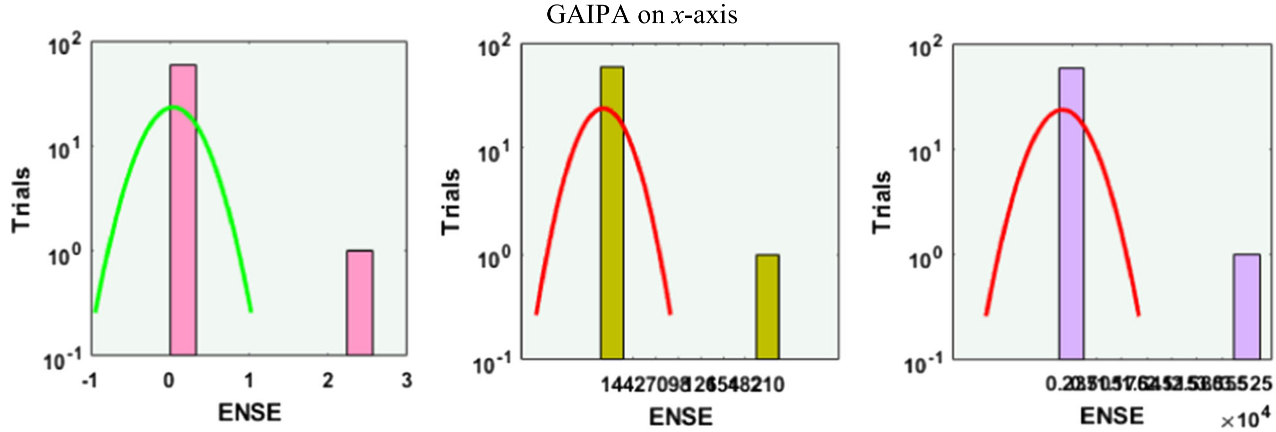

(a) Case-1: Hist ENSE values

(b) Case-2: Hist ENSE values

(c) Case-3: Hist ENSE values

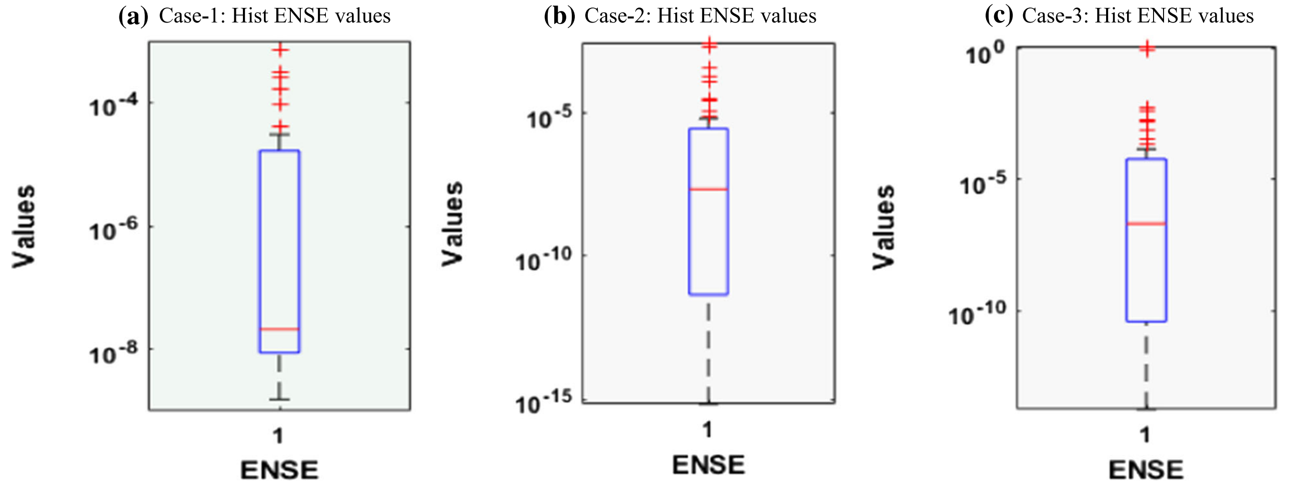

(d) Case-1: ENSE boxplot values

(e) Case-2: ENSE boxplot values

(f) Case-3: ENSE boxplot values

Fig. 5 Convergence plots of the MFMS-LEM using the ENSE together with the boxplots and histograms and 10 neurons

LEM. One may accomplish from these obtained results that a majority of the independent executions achieved very reasonable and accurate results for all the performance-based measures.

Table 1 Statistics values for the proposed FMWNN-GAIPA for each class of the novel designed MSMF-LEM

Method	Case	Mode	Solution of $S(y)$ based on statistical values									
			0.1	0.2	0.3	0.4	0.5	0.6	0.7	0.8	0.9	1
FMWNN-GAIPA	1	Min	4.8E−07	7.9E−07	1.9E−06	5.9E−06	1.4E−06	2.6E−06	9.5E−07	1.1E−08	1.0E−06	9.6E−07
		Med	3.8E−05	4.1E−05	3.4E−05	2.7E−05	2.4E−05	2.1E−05	2.0E−05	2.0E−05	1.9E−05	2.0E−05
		SIR	5.3E−04	6.4E−04	5.2E−04	3.8E−04	2.9E−04	2.3E−04	1.9E−04	1.3E−04	9.9E−05	7.6E−05
	2	Min	2.3E−06	3.5E−06	1.0E−07	4.7E−07	1.8E−06	2.7E−06	3.5E−06	1.2E−06	2.0E−06	1.1E−06
		Med	3.1E−05	3.0E−05	2.8E−05	2.5E−05	2.2E−05	2.0E−05	1.9E−05	1.9E−05	1.9E−05	1.7E−05
		SIR	4.6E−04	4.7E−04	3.1E−04	2.0E−04	1.4E−04	1.1E−04	7.6E−05	4.8E−05	2.6E−05	1.3E−05
	3	Min	1.2E−06	1.3E−07	7.3E−07	2.4E−06	2.8E−06	2.1E−06	1.5E−06	2.8E−06	2.7E−06	1.7E−06
		Med	3.2E−05	3.9E−05	3.9E−05	3.3E−05	2.5E−05	2.3E−05	2.3E−05	2.2E−05	2.5E−05	2.4E−05
		SIR	4.4E−04	6.0E−04	5.3E−04	4.7E−04	3.8E−04	3.2E−04	2.6E−04	2.1E−04	1.7E−04	1.3E−04
FMWNN-PSOIPA	1	Min	1.2E−06	1.6E−06	2.5E−06	4.7E−07	1.3E−06	4.6E−06	9.5E−06	2.1E−07	1.7E−07	3.2E−07
		Med	2.4E−05	3.1E−05	5.2E−05	5.9E−05	4.3E−05	6.2E−05	3.8E−05	1.0E−04	2.6E−05	3.1E−05
		SIR	3.1E−04	4.5E−04	4.1E−04	2.6E−04	1.9E−04	1.3E−04	2.9E−04	3.2E−04	1.0E−04	3.9E−05
	2	Min	1.9E−06	3.5E−06	1.1E−06	3.4E−07	2.6E−06	1.6E−06	2.4E−06	2.7E−06	3.2E−06	2.4E−06
		Med	1.2E−05	2.4E−05	1.7E−05	4.3E−05	3.1E−05	4.1E−05	5.1E−05	3.7E−05	2.8E−05	2.5E−05
		SIR	3.5E−04	2.9E−04	2.7E−04	1.3E−04	2.3E−04	2.4E−04	6.4E−05	3.5E−05	1.3E−05	2.6E−05
	3	Min	2.4E−06	2.3E−06	4.2E−06	3.5E−06	1.7E−06	3.2E−06	5.3E−06	7.1E−06	1.4E−06	2.1E−06
		Med	1.9E−05	2.7E−05	2.5E−05	2.2E−05	4.7E−05	4.5E−05	1.9E−05	3.5E−05	5.3E−05	1.3E−05
		SIR	3.9E−04	9.0E−04	4.2E−04	3.5E−04	2.6E−04	2.1E−04	4.4E−04	1.5E−04	2.6E−04	2.4E−04

For precision and accuracy studies further, the statistical operatives based on minimum (Min), median (Med), and semi-interquartile range (S.I.R) are calculated for 60 independent runs using the FMWNN-GAIPA and obtained outcome are tabulated in Table 1 for all cases of the novel MSMF-LES. The independent trials of the proposed FMWNN-GAIPA based on the Min for best trials, Med for median trials and S.I.R operator values are used for one-half of the difference of 3rd quartile and 1st quartile. The results of statistical observations as presented in Figs. 2, 3, 4 and 5, one can evidently decipher that the small, reliable Min, Med, S.D and S.I.R metrics are obtained consistently that validate the stability, accuracy and performance of the proposed FMWNN-GAIPA for each case of the novel designed MSMF-LEM.

The accuracy, convergence and stability of the proposed neuro-evolution-based methodology FMWNN-GAIPA is further examined through comparative studies with FMWNN optimized with global search efficacy of particle swarm optimization (PSO) algorithm aided with efficient fine tuning with IPA, i.e., FMWNN-PSOIPA for solving all three cases of MSMF-LEM for 60 number of autonomous trails. The procedure and parameter settings of PSO are adopted as given in the similar reported studies [34, 91], while the same setting of the parameters is used for IPA as incorporated for GAs. The results of statistical operatives based on Min, Med and SIR are calculated for FMWNN-PSOIPA on the similar procedure as incorporated for FMWNN-GAIPA for all three cases of MSMF-LEM and are tabulated in Table 1 for the same inputs. It can be seen that the values of Min lie around 10^{-7} to 10^{-6}, for all three cases of MSMF-LEM by FMWNN-PSOIPA, which is quite similar to FMWNN-GAIPA. Generally, no noticeable difference between the results involving GA and PSO but slight better accuracy is achieved by FMWNN-GAIPA. However, the said bit better performance of FMWNN-GAIPA is attained at the cost of 10% to 15% more computation complexity than that of FMWNN-PSOIPA.

5 Conclusions

The present study is about to introduce a mathematical model for the MSMF-LEM by using the sense of typical the multi-singular Lane–Emden model with multiple terms of fractional order, i.e., non-integer, derivatives. The fractional terms, shape factors and singular point details are also introduced in the designed system at origin three times, i.e., $y = 0$, $y^2 = 0$ and $y^3 = 0$. To observe the perfection and correctness of novel multi-fractional multi-singular Lane–Emden system, three different cases are formulated and solved with the prominent structure of ANNs together with global as well as local search capabilities of genetic algorithm and interior-point algorithms.

The proposed FMWNN-GAIPA is broadly applied on the novel multi-fractional multi-singular Lane–Emden system for three classes to demonstrate the constancy, convergence, accuracy and robustness. The comparison of the achieved numerical outcomes from the FMWNN-GAIPA with the true/exact results is presented with order of matching almost 5–7 decimals of accuracy level, which validates the exactness and efficiency of the FMWNN-GAIPA. Furthermore, statistical studies of the designed FMWNN-GAIPA on 60 runs show accurate and precise results consistently. Additionally, the computational efficiency of the design FMWNN-GAIPA can be improved further by use of different definitions of fractional derivative introduced recently in the literature for smooth, viable and functioning outcomes. Furthermore, the optimization procedure based on variant of particle swarm optimization algorithm can be a good alternative to improve the computational efficacy for learning of design variants of FMWNNs.

In the future work, one can extend the designed FMWNN-GAIPA via FMNEICS approach to be implemented to solve the linear/nonlinear stiff, singular and fractional as well as integer order models arising in different domains including atomic/plasma physics models [88–90], computational fluidic models [92–94], information security systems [95, 96] and biological models [97–101].

Declarations

Conflict of interest The authors declare that there is no conflict of interest regarding this work.

References

1. Momani S, Ibrahim RW (2008) On a fractional integral equation of periodic functions involving Weyl-Riesz operator in Banach algebras. J Math Anal Appl 339(2):1210–1219
2. Diethelm K, Ford NJ (2002) Analysis of fractional differential equations. J Math Anal Appl 265(2):229–248
3. Ibrahim RW, Momani S (2007) On the existence and uniqueness of solutions of a class of fractional differential equations. J Math Anal Appl 334(1):1–10
4. Yu F (2009) Integrable coupling system of fractional soliton equation hierarchy. Phys Lett A 373(41):3730–3733
5. Bonilla B, Rivero M, Trujillo JJ (2007) On systems of linear fractional differential equations with constant coefficients. Appl Math Comput 187(1):68–78
6. Sumelka W (2014) Fractional viscoplasticity. Mech Res Commun 56:31–36
7. Szymczyk M, Nowak M, Sumelka W (2020) Plastic strain localization in an extreme dynamic tension test of steel sheet in the framework of fractional viscoplasticity. Thin-Walled Struct 149:106522
8. Diethelm K, Freed AD (1999) On the solution of nonlinear fractional-order differential equations used in the modeling of viscoplasticity. In: Scientific computing in chemical engineering II. Springer, Berlin, pp 217–224
9. Chaudhary NI et al (2021) Design of multi innovation fractional LMS algorithm for parameter estimation of input nonlinear control autoregressive systems. Appl Math Model 93:412–425
10. Zhang Y, Sun H, Stowell HH, Zayernouri M, Hansen SE (2017) A review of applications of fractional calculus in Earth system dynamics. Chaos Solitons Fractals 102:29–46
11. Muhammad Y et al (2021) Design of fractional evolutionary processing for reactive power planning with FACTS devices. Sci Rep 11(1):1–29
12. Daou RAZ, El Samarani F, Yaacoub C, Moreau X (2020) Fractional derivatives for edge detection: application to road obstacles. In: Smart cities performability, cognition, & security. Springer, Cham, pp 115–137
13. Khan MW et al (2020) A New Fractional Particle Swarm Optimization with Entropy Diversity Based Velocity for Reactive Power Planning. Entropy 22(10):1112
14. Evans RM, Katugampola UN, Edwards DA (2017) Applications of fractional calculus in solving Abel-type integral equations: Surface–volume reaction problem. Comput Math Appl 73(6):1346–1362
15. Khan NH et al (2020) Design of fractional particle swarm optimization gravitational search algorithm for optimal reactive power dispatch problems. IEEE Access 8:146785–146806
16. Torvik PJ, Bagley RL (1984) On the appearance of the fractional derivative in the behavior of real materials. J Appl Mech 51(2):294–298
17. Chaudhary NI et al (2020) An innovative fractional order LMS algorithm for power signal parameter estimation. Appl Math Model 83:703–718
18. Matlob MA, Jamali Y (2019) The concepts and applications of fractional order differential calculus in modeling of viscoelastic systems: a primer. Crit Rev™ Biomed Eng 47(4)
19. Muhammad Y et al (2020) Design of fractional swarm intelligent computing with entropy evolution for optimal power flow problems. IEEE Access 8:111401–111419
20. Engheia N (1997) On the role of fractional calculus in electromagnetic theory. IEEE Antennas Propag Mag 39(4):35–46
21. Sabir Z et al (2021) Design of Morlet wavelet neural network for solving the higher order singular nonlinear differential equations. Alex Eng J 60(6):5935–5947
22. Aman S, Khan I, Ismail Z, Salleh MZ (2018) Applications of fractional derivatives to nanofluids: exact and numerical solutions. Math Model Nat Phenomena 13(1):2
23. Masood Z et al (2020) Design of fractional order epidemic model for future generation tiny hardware implants. Futur Gener Comput Syst 106:43–54
24. Yang XJ, Machado JT, Cattani C, Gao F (2017) On a fractal LC-electric circuit modeled by local fractional calculus. Commun Nonlinear Sci Numer Simul 47:200–206
25. Bukhari AH et al (2020) Fractional neuro-sequential ARFIMA-LSTM for financial market forecasting. IEEE Access 8:71326–71338
26. Dabiri A, Butcher EA, Nazari M (2017) Coefficient of restitution in fractional viscoelastic compliant impacts using fractional Chebyshev collocation. J Sound Vib 388:230–244
27. Zameer A et al (2020) Fractional-order particle swarm based multi-objective PWR core loading pattern optimization. Ann Nucl Energy 135:106982
28. Onal M, Esen A (2020) A Crank-Nicolson approximation for the time fractional Burgers equation. Appl Math Nonlinear Sci 5(2):177–184

29. Khan ZA, Zubair S, Chaudhary NI et al (2020) Design of normalized fractional SGD computing paradigm for recommender systems. Neural Comput Appl 32:10245–10262. https://doi.org/10.1007/s00521-019-04562-6
30. Băleanu D, Lopes AM (eds) (2019) Applications in Engineering, Life and Social Sciences. Walter de Gruyter GmbH & Co KG. https://doi.org/10.1515/9783110571905.
31. Kabra S et al (2020) The Marichev-Saigo-Maeda fractional calculus operators pertaining to the generalized k-struve function. Appl Math Nonlinear Sci 2:593–602
32. Sun H, Zhang Y, Baleanu D, Chen W, Chen Y (2018) A new collection of real world applications of fractional calculus in science and engineering. Commun Nonlinear Sci Numer Simul 64:213–231
33. Muhammad Y, Khan R, Ullah F et al (2020) Design of fractional swarming strategy for solution of optimal reactive power dispatch. Neural Comput & Applic 32:10501–10518. https://doi.org/10.1007/s00521-019-04589-9
34. Umar M et al (2021) Neuro-swarm intelligent computing paradigm for nonlinear HIV infection model with CD4+ T-cells. Math Comput Simul 188:241–253
35. Guerrero-Sánchez Y (2020) Solving a class of biological HIV infection model of latently infected cells using heuristic approach. Discret Contin Dyn Syst S. https://doi.org/10.3934/dcdss.2020431
36. Sabir Z et al (2020) Integrated intelligent computing with neuro-swarming solver for multi-singular fourth-order nonlinear Emden-Fowler equation. Comput Appl Math 39(4):1–18
37. He JH, Ji FY (2019) Taylor series solution for Lane-Emden equation. J Math Chem 57(8):1932–1934
38. Sabir Z et al (2020) Heuristic computing technique for numerical solutions of nonlinear fourth order Emden-Fowler equation. Math Comput Simul 178:534–548
39. Sabir Z et al (2021) A novel design of fractional Meyer wavelet neural networks with application to the nonlinear singular fractional Lane-Emden systems. Alex Eng J 60(2):2641–2659
40. Abdelkawy MA et al (2020) Numerical investigations of a new singular second-order nonlinear coupled functional Lane-Emden model. Open Physics 18(1):770–778
41. Sabir Z et al (2021) Fractional Mayer Neuro-swarm heuristic solver for multi-fractional Order doubly singular model based on Lane-Emden equation. Fractals. https://doi.org/10.1142/S0218348X2140017X
42. Sabir Z et al (2021) Neuro-swarms intelligent computing using Gudermannian kernel for solving a class of second order Lane-Emden singular nonlinear model [J]. AIMS Math 6(3):2468–2485
43. Farooq MU (2019) Noether-Like operators and first integrals for generalized systems of Lane-Emden equations. Symmetry 11(2):162
44. Sabir Z et al (2020) Novel design of Morlet wavelet neural network for solving second order Lane-Emden equation. Math Comput Simul 172:1–14
45. Hadian-Rasanan AH, Rahmati D, Gorgin S, Parand K (2020) A single layer fractional orthogonal neural network for solving various types of Lane–Emden equation. New Astronomy 75:101307
46. Sabir Z et al (2020) FMNEICS: fractional Meyer neuro-evolution-based intelligent computing solver for doubly singular multi-fractional order Lane-Emden system. Comput Appl Math 39(4):1–18
47. Touchent KA, Hammouch Z, Mekkaoui T (2020) A modified invariant subspace method for solving partial differential equations with non-singular kernel fractional derivatives. Appl Math Nonlinear Sci 5(2):35–48
48. Umar M et al (2020) A stochastic numerical computing heuristic of SIR nonlinear model based on dengue fever. Results Phys 103585
49. Sabir Z et al (2020) A Neuro-Swarming Intelligence-Based Computing for Second Order Singular Periodic Non-linear Boundary Value Problems. Front Phys 8:224
50. Umar M et al (2020) A Stochastic Intelligent Computing with Neuro-Evolution Heuristics for Nonlinear SITR System of Novel COVID-19 Dynamics. Symmetry 12(10):1628
51. Raja MAZ et al (2018) A new stochastic computing paradigm for the dynamics of nonlinear singular heat conduction model of the human head. Eur Phys J Plus 133(9):1–21
52. Umar M et al (2019) Intelligent computing for numerical treatment of nonlinear prey–predator models. Appl Soft Comput 80:506–524
53. Sabir, Z.et al, (2018) Neuro-heuristics for nonlinear singular Thomas-Fermi systems. Appl Soft Comput 65:152–169
54. Umar M et al (2020) A stochastic computational intelligent solver for numerical treatment of mosquito dispersal model in a heterogeneous environment. Eur Phys J Plus 135(7):1–23
55. Umar M et al (2020) Stochastic numerical technique for solving HIV infection model of CD4+ T cells. Eur Phys J Plus 135(6):403
56. Pandey K et al (2020) Artificial Neural Network Optimized with a Genetic Algorithm for Seasonal Groundwater Table Depth Prediction in Uttar Pradesh, India . Sustainability 12(21):8932
57. Mouassa S, Jurado F, Bouktir T et al (2020) Novel design of artificial ecosystem optimizer for large-scale optimal reactive power dispatch problem with application to Algerian electricity grid. Neural Comput Appl. https://doi.org/10.1007/s00521-020-05496-0
58. Ghalandari M et al (2019) Aeromechanical optimization of first row compressor test stand blades using a hybrid machine learning model of genetic algorithm, artificial neural networks and design of experiments. Eng Appl Comput Fluid Mech 13(1):892–904
59. Ahmad I et al (2020) Integrated neuro-evolution-based computing solver for dynamics of nonlinear corneal shape model numerically. Neural Comput Applic. https://doi.org/10.1007/s00521-020-05355-y
60. Najafi B, Faizollahzadeh Ardabili S, Shamshirband S, Chau KW, Rabczuk T (2018) Application of ANNs, ANFIS and RSM to estimating and optimizing the parameters that affect the yield and cost of biodiesel production. Eng Appl Comput Fluid Mech 12(1):611–624
61. Mehmood A et al (2020) Design of nature-inspired heuristic paradigm for systems in nonlinear electrical circuits. Neural Comput Appl 32(11):7121–7137
62. Taormina R, Chau KW (2015) ANN-based interval forecasting of streamflow discharges using the LUBE method and MOFIPS. Eng Appl Artif Intell 45:429–440
63. Mehmood A, Shi P et al (2021) Design of backtracking search heuristics for parameter estimation of power signals. Neural Comput Appl 33:1479–1496. https://doi.org/10.1007/s00521-020-05029-9
64. Kazemi SMR, Minaei Bidgoli B, Shamshirband S, Karimi SM, Ghorbani MA, Chau KW, Kazem Pour R (2018) Novel genetic-based negative correlation learning for estimating soil temperature. Eng Appl Comput Fluid Mech 12(1):506–516
65. Mehmood A, Zameer A, Chaudhary NI et al (2020) Design of meta-heuristic computing paradigms for Hammerstein

identification systems in electrically stimulated muscle models. Neural Comput Applic 32:12469–12497. https://doi.org/10.1007/s00521-020-04701-4
66. Wu CL, Chau KW (2013) Prediction of rainfall time series using modular soft computing methods. Eng Appl Artif Intell 26(3):997–1007
67. Raja MAZ, Chaudhary NI, Ahmed Z, Rehman AU, Aslam MS (2019) A novel application of kernel adaptive filtering algorithms for attenuation of noise interferences. Neural Comput Appl 31(12):9221–9240
68. Raja MAZ, Manzar MA, Samar R (2015) An efficient computational intelligence approach for solving fractional order Riccati equations using ANN and SQP. Appl Math Model 39(10–11):3075–3093
69. Zúñiga-Aguilar CJ, Romero-Ugalde HM, Gómez-Aguilar JF, Escobar-Jiménez RF, Valtierra-Rodríguez M (2017) Solving fractional differential equations of variable-order involving operators with Mittag-Leffler kernel using artificial neural networks. Chaos Solitons Fract 103:382–403
70. Ahmad I et al (2019) Novel applications of intelligent computing paradigms for the analysis of nonlinear reactive transport model of the fluid in soft tissues and microvessels. Neural Comput Appl 31(12):9041–9059
71. Artar M, Daloğlu AT (2018) Optimum weight design of steel space frames with semi-rigid connections using harmony search and genetic algorithms. Neural Comput Appl 29(11):1089–1100
72. Adánez JM, Al-Hadithi BM, Jiménez A (2019) Multidimensional membership functions in T-S fuzzy models for modelling and identification of nonlinear multivariable systems using genetic algorithms. Appl Soft Comput 75:607–615
73. Hassan A, Kamran M, Illahi A, Zahoor RMA (2019) Design of cascade artificial neural networks optimized with the memetic computing paradigm for solving the nonlinear Bratu system. Eur Phys J Plus 134(3):122
74. Flórez CAC, Rosário JM, Amaya D (2018) Control structure for a car-like robot using artificial neural networks and genetic algorithms. Neural Comput Appl 20(2020):1–14
75. Zameer A et al (2019) Bio-inspired heuristics for layer thickness optimization in multilayer piezoelectric transducer for broadband structures. Soft Comput 23(10):3449–3463
76. Raja MAZ et al (2019) Design of hybrid nature-inspired heuristics with application to active noise control systems. Neural Comput Appl 31(7):2563–2591
77. Akbar S et al (2017) Design of bio-inspired heuristic techniques hybridized with sequential quadratic programming for joint parameters estimation of electromagnetic plane waves. Wireless Pers Commun 96(1):1475–1494
78. Raja MAZ, Khan JA, Zameer A, Khan NA, Manzar MA (2019) Numerical treatment of nonlinear singular Flierl-Petviashivili systems using neural networks models. Neural Comput Appl 31(7):2371–2394
79. Jamal R et al (2019) Hybrid Bio-Inspired Computational Heuristic Paradigm for Integrated Load Dispatch Problems Involving Stochastic Wind. Energies 12(13):2568
80. Raja MAZ et al (2017) Design of bio-inspired heuristic technique integrated with interior-point algorithm to analyze the dynamics of heartbeat model. Appl Soft Comput 52:605–629
81. Bertocchi C, Chouzenoux E, Corbineau MC, Pesquet JC, Prato M (2020) Deep unfolding of a proximal interior point method for image restoration. Inverse Probl 36(3):034005
82. Raja MAZ et al (2019) Bio-inspired heuristics hybrid with sequential quadratic programming and interior-point methods for reliable treatment of economic load dispatch problem. Neural Comput Appl 31(1):447–475
83. Jiang H, Kathuria T, Lee YT, Padmanabhan S, Song Z (2020) A faster interior point method for semidefinite programming. In: 2020 IEEE 61st annual symposium on foundations of computer science (FOCS), 2020, pp 910–918. https://doi.org/10.1109/FOCS46700.2020.00089
84. Raja MAZ, Aslam MS, Chaudhary NI, Khan WU (2018) Bio-inspired heuristics hybrid with interior-point method for active noise control systems without identification of secondary path. Front Inf Technol Electron Eng 19(2):246–259
85. Dueri D, Açıkmeşe B, Scharf DP, Harris MW (2017) Customized real-time interior-point methods for onboard powered-descent guidance. J Guid Control Dyn 40(2):197–212
86. Mangoni D, Tasora A, Garziera R (2018) A primal–dual predictor–corrector interior point method for non-smooth contact dynamics. Comput Methods Appl Mech Eng 330:351–367
87. Wambacq J, Maes K, Rezayat A, Guillaume P, Lombaert G (2019) Localization of dynamic forces on structures with an interior point method using group sparsity. Mech Syst Signal Process 115:593–606
88. Raja MAZ, Shah FH, Tariq M, Ahmad I (2018) Design of artificial neural network models optimized with sequential quadratic programming to study the dynamics of nonlinear Troesch's problem arising in plasma physics. Neural Comput Appl 29(6):83–109
89. Ahmed SI et al (2020) A new heuristic computational solver for nonlinear singular Thomas-Fermi system using evolutionary optimized cubic splines. Eur Phys J Plus 135(1):1–29
90. Bukhari AH et al (2020) Design of a hybrid NAR-RBFs neural network for nonlinear dusty plasma system. Alex Eng J 59(5):3325–3345
91. Umar M et al (2021) Integrated neuro-swarm heuristic with interior-point for nonlinear SITR model for dynamics of novel COVID-19. Alex Eng J 60(3):2811–2824
92. Assad A et al (2021) Nanoscale heat and mass transport of magnetized 3-D chemically radiative hybrid nanofluid with orthogonal/inclined magnetic field along rotating sheet, Case Studies in Thermal Engineering, Volume 26. ISSN 101193:2214–3157. https://doi.org/10.1016/j.csite.2021.101193
93. Ayub A et al (2021) Interpretation of infinite shear rate viscosity and a nonuniform heat sink/source on a 3D radiative cross nanofluid with buoyancy assisting/opposing flow. Heat Transfer 50(5):4192–4232
94. Sabir Z, Ali MR, Raja MAZ et al (2021) Computational intelligence approach using Levenberg–Marquardt backpropagation neural networks to solve the fourth-order nonlinear system of Emden–Fowler model. Eng Comput. https://doi.org/10.1007/s00366-021-01427-2
95. Masood Z et al (2019) Design of a mathematical model for the Stuxnet virus in a network of critical control infrastructure. Comput Secur 87:101565
96. Masood Z et al (2018) Design of epidemic computer virus model with effect of quarantine in the presence of immunity. Fund Inform 161(3):249–273
97. Elsonbaty A, et al (2021) Dynamical analysis of a novel discrete fractional sitrs model for COVID-19. Fractals Article ID:2140035
98. Cheema TN et al (2020) Intelligent computing with Levenberg–Marquardt artificial neural networks for nonlinear system of COVID-19 epidemic model for future generation disease control. Eur Phys J Plus 135(11):1–35

99. Guerrero Sánchez Y et al (2020) Analytical and approximate solutions of a novel nervous stomach mathematical model. Discrete Dyn Nat Soc 2020:1–9
100. Sabir Z et al (2020) Numerical investigations to design a novel model based on the fifth order system of Emden-Fowler equations. Theor Appl Mech Lett 10(5):333–342
101. Guerrero Sánchez Y et al (2020) Design of a nonlinear SITR fractal model based on the dynamics of a novel coronavirus (COVID). Fractals 28(8):1–6

Publisher's Note Springer Nature remains neutral with regard to jurisdictional claims in published maps and institutional affiliations.